SI Appendix

Supporting information for "Hydrophobic catalysis and a potential biological role of DNA unstacking induced by environment effects"

Bobo Feng, Robert P. Sosa, Anna K. F. Mårtensson, Kai Jiang, Alex Tong, Kevin D. Dorfman, Masayuki Takahashi, Per Lincoln, Carlos J. Bustamante, Fredrik Westerlund, Bengt Nordén

Contents

1. Materials and methods 2
1a. Sample preparation for intercalation, CD, LD, and hyperchromicity 2
1b. Fluorescence and absorption spectroscopy 2
1c. Glyoxal reaction 2
1d. CD and LD measurements 3
1e. Single DNA manipulation using optical tweezers 4
1f. Single DNA observation in nano-channels 4
2. CD and hyperchromicity of DNA in PEG and diglyme 6
3. Structure of ruthenium complex 7
4. Thread-intercalation kinetics in PEG-400 8
5. Thread-intercalation in dioxane, diglyme, glycerol, PVA, and dextran 14
6. Glyoxal reactions 17
7. Linear dichroism of DNA in diglyme, glycerol, PEG and TE buffer 19
8. Hyperchromicity - theory 23
9. Tables 24
9. References 25

www.pnas.org/cgi/doi/10.1073/pnas.1909122116

1. Materials and methods

The concentrations used for intercalation experiments in this article are up to 40 % (w/w) for PEG-400, and up to 20 % (w/w) for diglyme. Higher concentrations of PEG cause the rate of intercalation to be too fast to be practically measurable and thus less meaningful here. Diglyme was used as a substitute for PEG in the optical tweezer and LD experiments. PEG has an unsuitable refractive index for the optical tweezers setup, and its higher viscosity was found difficult to match using a reasonable concentration of glycerol.

1a. Sample preparation for intercalation, CD, LD, and hyperchromicity

Calf thymus DNA fibres type I (Sigma-Aldrich) was dissolved in double distilled water overnight under gentle stirring. The resulting solution was filtered twice through a 50 µm nitrocellulose filter, resulting in a 1 cm absorbance of about 100 at 260 nm. Concentration was determined using $\varepsilon_{260\ nm}$ = 6 600 $M^{-1}cm^{-1}$ per average nucleotide.

Polyethylene glycol (polydisperse, average MW = 400, Rectapur, VWR), diglyme (diethylene glycol dimethyl ether, 99%, Sigma-Aldrich), and dioxane (p.a., Merck) were mixed with TE buffer (pH 8) containing 10 mM Tris (Trizma base, ≥ 99.7 %, Sigma) and 1 mM EDTA (≥ 99 %, Sigma-Aldrich). Solid sodium chloride (≥ 99.5 %, Sigma-Aldrich) was weighed on an analytical balance (Sartorius MSE225S) and added in the last step of sample preparation to avoid being diluted by the addition of PEG and diglyme.

Homochiral pure ruthenium bicomplex ΔΔ-[µ-bidppz(phen)$_4$Ru$_2$]$^{4+}$ ($\varepsilon_{408\ nm}$ = 74 000 $M^{-1}cm^{-1}$) was synthesized as described previously (1).

1b. Fluorescence and absorption spectroscopy

Fluorescence emission (40 µM nucleotides, 2 µM ruthenium complex) was measured on a Varian Cary Eclipse fluorometer (0.2-0.5 s averaging time, excitation 450 nm, emission 630 nm, 10 nm slits and 750-800 V photomultiplier voltage) using a 1 cm quartz cell at 50 °C under magnetic stirring.

The dumbbell-shaped ruthenium bi-complex ΔΔ-[µ-bidppz(phen)4Ru2]$^{4+}$ (Fig S5) was used to probe for unstacked holes between nucleobases. The complex exhibits very slow threading intercalation into native ctDNA in pure TE buffer due to its sterically obstructive shape. Furthermore, the so-called "molecular light switch effect" ensures that fluorescence is observed when the complex is intercalated into the hydrophobic interior of DNA, while fluorescence is effectively quenched in an aqueous environment (1-3). The reaction yield is calculated by normalizing the observed fluorescence with respect to the final intensity when no further reaction is observed (for fitting of data to a biexponential model, see section 3).

Absorbance spectra were recorded using a Varian Cary Bio 50 spectrophotometer with a 1 cm quartz cell, except for melting curves which were done using a Cary 4000 and a Cary 5000 equipped with a multicell heating block and under magnetic stirring.

1c. Glyoxal reaction

Glyoxal (Sigma Aldrich, ~8.8 M solution in water) is a specific reagent for single DNA strands by irreversibly forming an adduct with exo-cyclic amino groups of unpaired guanines. To avoid cross-reaction between glyoxal and the amine function in Tris, double distilled water at pH 7.5 with 50 mM NaCl was used instead of TE buffer. Absorbance spectra were taken at timed intervals until no further progress could be determined. The cell was heated to 50 °C using a separate water bath except for when spectra were measured (less than one minute per spectrum).

1d. CD and LD measurements

Circular dichroism was measured using an Applied Photophysics Chirascan spectropolarimeter and a 1 cm quartz cell with the sample holder thermostat set to 50 °C, spectra were measured using the average of 4 passes at 5 minutes per pass.

Linear dichroism was measured using a Chirascan modified for LD measurements (100 kHz modulation frequency) with a custom built 30 mm diameter quartz Couette cell with rotating outer cylinder and fixed inner cylinder with a 0.5 mm gap. Measurements were made at radial beam incidence providing the LD^r (LD divided by absorbance of the isotropic solution) as:

$$LD^r = \frac{(A_X - A_Y)}{A_{iso}} = 3\ O(\alpha)\ S(G)$$

with A_X and A_Y the absorbancies measured with linearly polarized light parallel with the flow lines (axis X) and parallel with the cylinder axis (Y) of the flow cell, respectively, and A_{iso} being the (isotropic) absorbance of the solution at rest. $A_i = \varepsilon_i\ C\ d$, i = X and Y, with the corresponding extinction coefficient and C concentration and d optical pathlength. Since $A_{iso} = \varepsilon_{iso}\ C\ d$, both C and d vanish in LD^r, which factorizes as shown by the second sign of equality into an orientation factor $S(G)$ dependent on flow gradient and an optical factor, $O(\alpha) = \frac{1}{2} 3\cos^2\alpha - 1$, with α the angle between the light-absorbing transition moment and the local DNA helix axis (with several overlapping transitions O is a weighted average over their absorptions) (4).

For a worm-like coil the LD^r is directly proportional to the ratio P/L, of the persistence length P and the contour length L (4-6).

$$LD^r = \frac{A_X - A_Y}{A_{iso}} = 3O(\alpha)\frac{2}{3}\frac{P}{L}\beta^2 K$$

Here β is the "reduced gradient" $\beta = M[\eta]\eta_0 G/NkT$ where M is the molecular weight and $[\eta]$ and η_0 intrinsic and solvent viscosity, respectively. $G = dv_x/d_z$ (v_x flow velocity) is the shear flow gradient (s^{-1}), N the Avogadro number, k Boltzmann's constant and T the temperature. K is a constant related to the eigenvalues λ_i of the Zimm matrix, dependent on to which degree the DNA behaves as a free-draining coil.

Viscosities were measured at room temperature (thermostat set to 22 °C) using a Paar Physica MCR 500 rheometer equipped with a measuring cone (50 mm in diameter, 0.6 mL sample volume, 200 rpm). To a good approximation, for two DNA samples A and B referring to the same viscosity and contour length L, the ratio of persistence lengths is directly given from the LD ratio:

$$LD^r_A / LD^r_B = P_A / P_B$$

As B conformation maintains for DNA in up to at least 25 % glycerol (7), and if 50 nm is taken as a reasonable value for $P_{glycerol}$, the persistence length in diglyme is simply $P_{diglyme} = (LD^r_{diglyme}/LD^r_{glycerol}) \times 50$ nm.

1e. Single DNA manipulation using optical tweezers

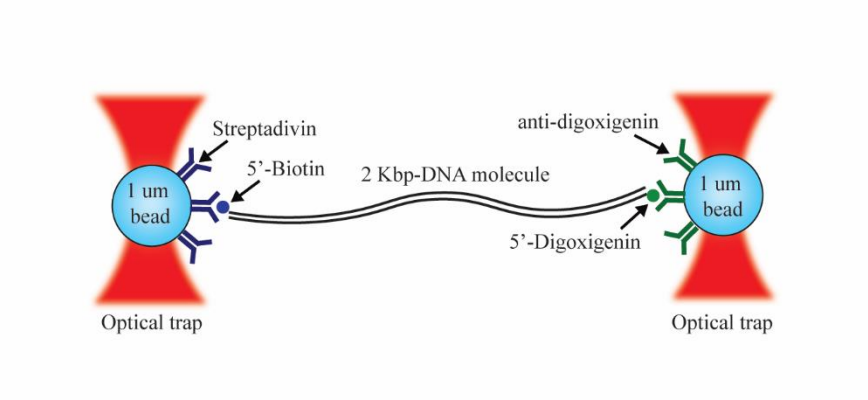

A dual-trap high resolution optical tweezers setup was used to manipulate single DNA molecules (8, 9). A 2 kbp-long DNA was produced by PCR, using a digoxigenin-labelled forward primer, a biotin-labelled reverse primer (IDT), and Phusion DNA polymerase (NEB), followed by gel purification of the product. The biotin end of DNA was attached to the optical trap polystyrene bead via biotin/streptavidin bridge, while the digoxigenin end was attached to a second optical trap polystyrene bead through a digoxigenin/anti-digoxigenin antibody association. Pulling experiments were performed in TE buffer (10 mM Tris-HCl pH 8.0, 0.1 mM EDTA and 150 mM NaCl) with 10 mM of sodium azide to avoid photodamage (10). Experiments were carried out using a trap stiffness of $\kappa \sim 0.75$ pN/nm for all conditions tested and κ was estimated using the power spectrum method (9). We performed similar DNA pulling experiments but also in the presence of 10 and 20 % (w/v) diglyme. For glyoxal control, DNA was pre-incubated in 20 % diglyme, 20 mM glyoxal, and 50 mM NaCl at room temperature for 1 hour.

We fitted DNA pulling curves below 30-35 pN to a modified extensible worm like chain (eWLC) model of polymer statistics (11):

$$\frac{FP}{k_B T} = \frac{1}{4}\left(1 - \frac{x(F)}{L} + \frac{F}{S}\right)^{-2} - \frac{1}{4} + \frac{x(F)}{L} - \frac{F}{S} - 0.8\left(\frac{x(F)}{L} - \frac{F}{S}\right)^{2.15}$$

Where P is the DNA persistent length (nm), S is the stretch modulus (pN) and L is the contour length (nm). DNA pulling curves were analyzed using a custom MATLAB code designed in Bustamante Lab.

1f. Single DNA observation in nano-channels

λ-DNA (48.5 kb, Roche) was pre-stained with YOYO-1 (Invitrogen). To minimize the effect of YOYO-1 on DNA conformation, a ratio of 1 dye molecule per 50 base pairs was used (12). Pre-stained DNA was then mixed with Polyethylene glycol 400 (VWR) and incubated at 4 °C for at least 1 hour. The mixtures were then introduced into the nanofluidic system and equilibrated for 60 s before image capture. The DNA concentration was 5 μM (base pairs) in all samples. The buffer used was 0.5 × TE (5 mM Tris and 0.5 mM EDTA, pH 7.5) with or without 150 mM NaCl, respectively.

The single DNA molecule experiments were performed in nanochannels with the dimensions 100 × 150 nm^2, fabricated using a nanofabrication protocol described elsewhere (13). The channel system consists of a pair of feeding channels (micro-size), spanned by a set of parallel nanochannels. The sample is loaded into the channel system from one of the four reservoirs that are connected to the feeding channels. Flow is used to move the single molecules into the nanochannels by applying N_2 pressure.

An epifluorescence microscope (Zeiss AxioObserver.Z1) equipped with a Photometrics Evolve EMCCD camera, a 63× oil immersion TIRF objective (NA = 1.46) and a 1.6× optovar from Zeiss was used to image the DNA molecules. Using the microscopy imaging software ZEN, 50 subsequent images were recorded with an exposure time of 100 ms. Data analysis was performed using a custom-written MATLAB-based software. Microscopy image stacks were used as input to the program. Images were first binarized by thresholding with a global average plus one-fold of standard deviation. Taking advantage of the high contrast of the YOYO-stained DNA fluorescence images, regions with higher brightness were directly considered as DNA objects without additional image filtering. Finally, the lengths of the DNA molecules were extracted by identifying the longest axis of the objects and the length was measured. More than 50 DNA molecules were analyzed for each sample concentration.

2. CD and hyperchromicity of DNA in PEG and diglyme

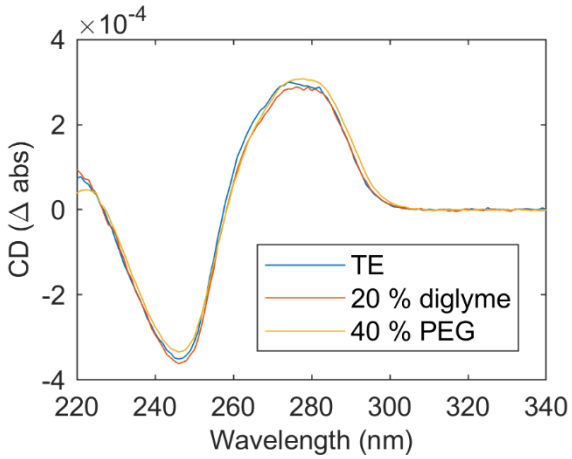

Fig. S1. Circular dichroism (CD) spectra confirm that B-DNA conformation is unchanged in presence of PEG and diglyme compared to in TE buffer.

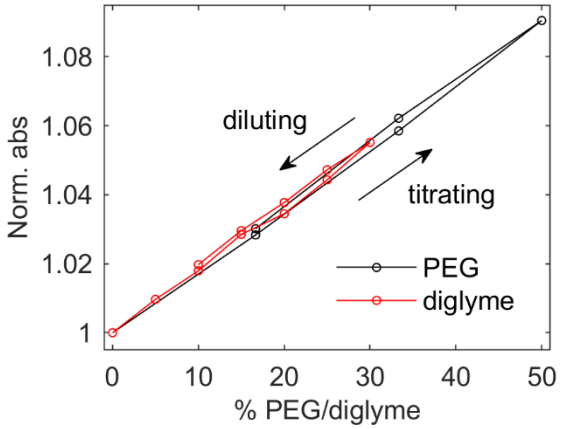

Fig. S2. Titrations with PEG and diglyme, and subsequent dilution with buffer, show that DNA exhibits a modest, immediately reversible hyperchromicity (absorbance at 260 nm) consistent with unstacking of bases. DNA absorbance peak at 260 nm remains unchanged (absorbance spectra in Fig. SI-8-9).

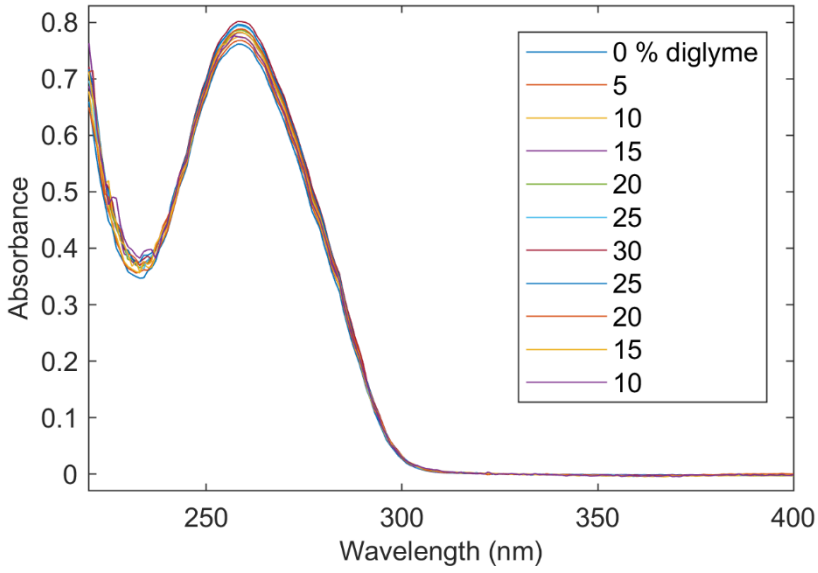

Fig. S3. Hyperchromicity of DNA obtained by titrating with diglyme up to 30 % (w/w) and subsequent dilution with TE buffer down to 10 %. The 260 nm DNA peak does not shift. The dilution factor of DNA has been accounted for.

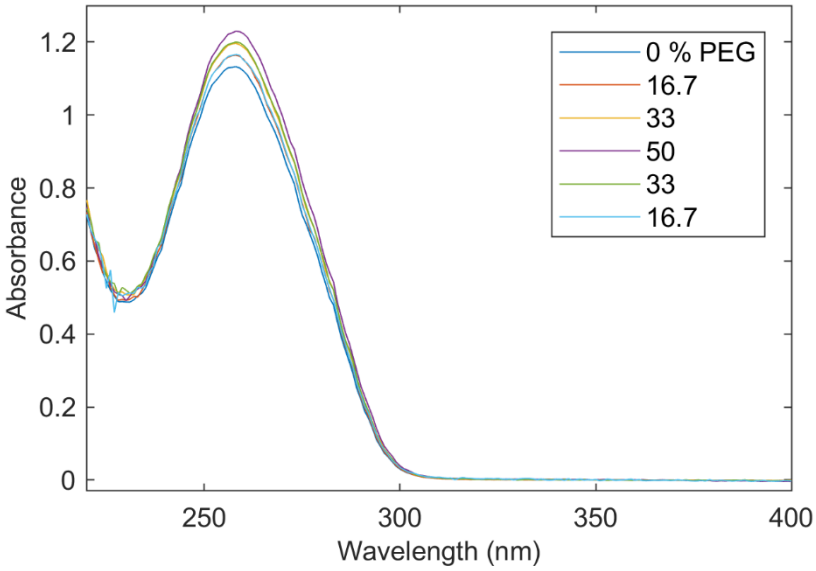

Fig. S4. Like Fig. S4 but with PEG up to 50 % (w/w).

3. Structure of ruthenium complex

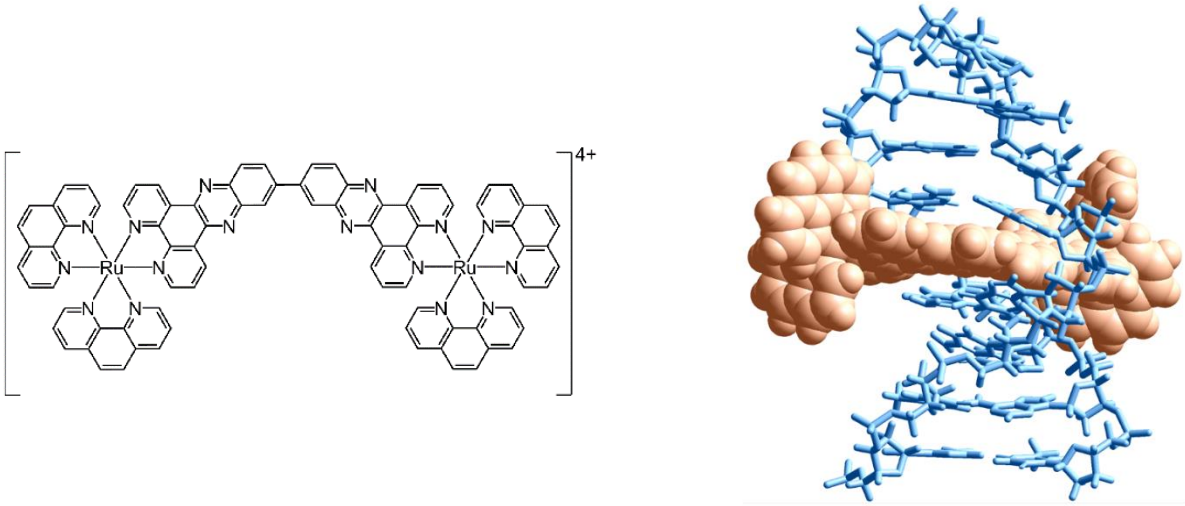

Fig. S5. Structure of the ruthenium bi-complex [μ-bidppz(phen)$_4$Ru$_2$]$^{4+}$ and a rendering of the complex thread-intercalated into DNA. Unlike conventional DNA intercalation, one of the bulky head groups must thread itself through the stack of nucleobases, requiring the appearance of a hole of significant size.

4. Thread-intercalation kinetics in PEG-400

Calculating intercalation yield through normalization of fluorescence intensity:

$$Y(t) = \frac{I(t) - I_0}{I_{t=\infty} - I_0}$$

Bi-exponential model:

$$Y(t) = 1 - Ae^{-kt} - (1 - A)e^{-mt}$$

Least-squares fitted parameters:

300 mM NaCl	PEG concentration (% w/w)				
	40	30	20	10	0
A	*	0.8586	0.795	0.7505	0.5995
k	*	0.1468	0.04154	0.0333	0.01685
m	*	0.04412	0.005336	0.004485	0.00422

* Not measurable due to DNA precipitation

225 mM NaCl	PEG concentration (% w/w)				
	40	30	20	10	0
A	0.7174	0.8447	0.7456	0.7199	0.5742
k	0.568	0.1499	0.06077	0.03271	0.01802
m	0.06265	0.04203	0.0101	0.003323	0.00354

150 mM NaCl	PEG concentration (% w/w)				
	40	30	20	10	0
A	0.7896	0.8616	0.78	0.641	0.4191
k	0.5647	0.1643	0.05018	0.03503	0.01731
m	0.06033	0.01677	0.005473	0.004954	0.005129

75 mM NaCl	PEG concentration (% w/w)				
	40	30	20	10	0
A	0.805	0.8252	0.8084	0.6162	0.5379
k	0.5794	0.1644	0.05233	0.03374	0.01749
m	0.04754	0.01784	0.008679	0.005129	0.003517

Actual fits (visualized in MATLAB R2017b):

0 % PEG, 75 mM NaCl

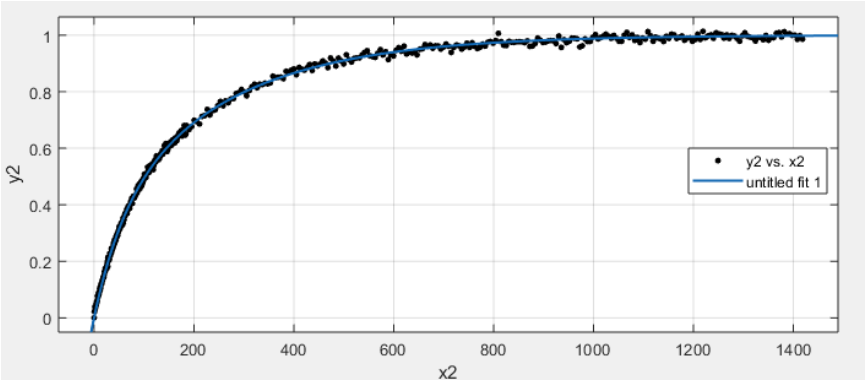

0 % PEG, 150 mM NaCl

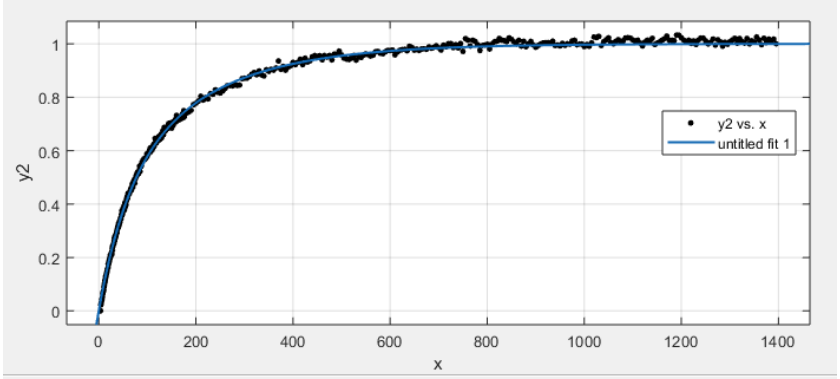

0 % PEG, 225 mM NaCl

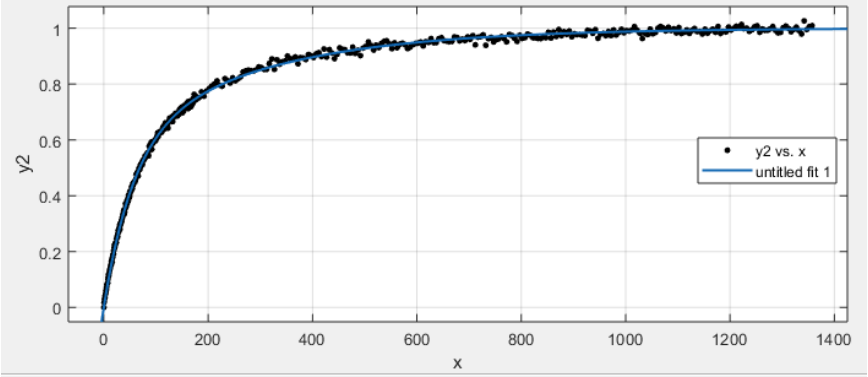

0 % PEG, 300 mM NaCl

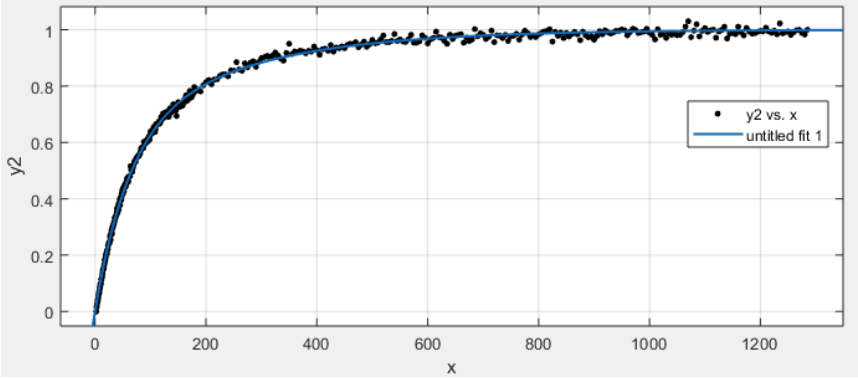

10 % PEG, 75 mM NaCl

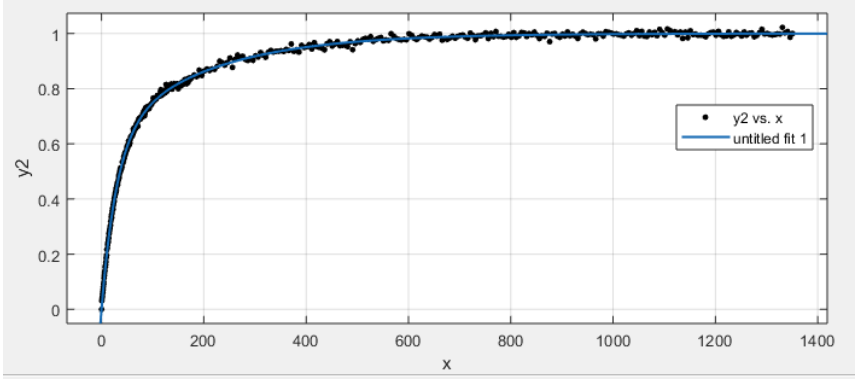

10 % PEG, 150 mM NaCl

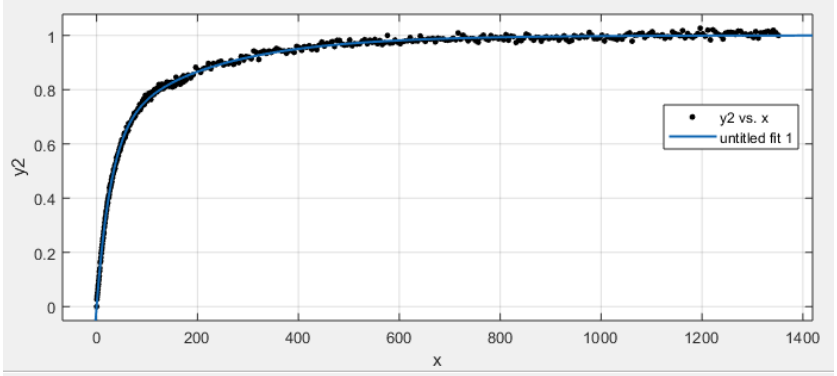

10 % PEG, 225 mM NaCl

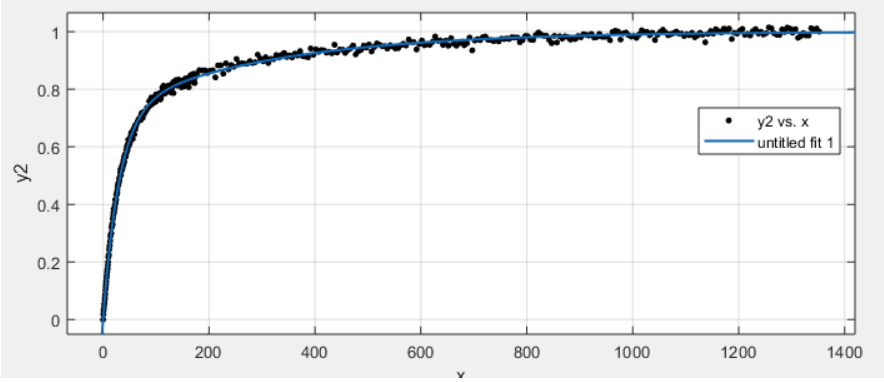

10 % PEG, 300 mM NaCl

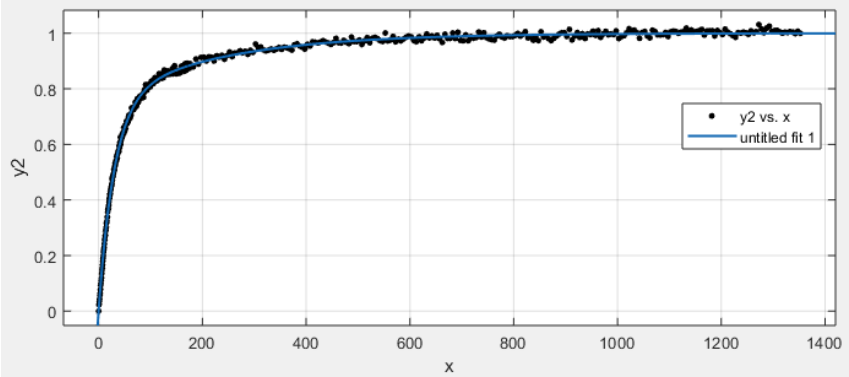

20 % PEG, 75 mM NaCl

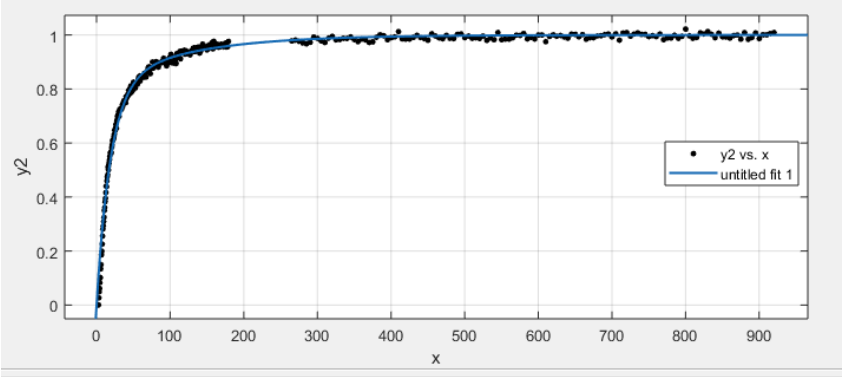

20 % PEG, 150 mM NaCl

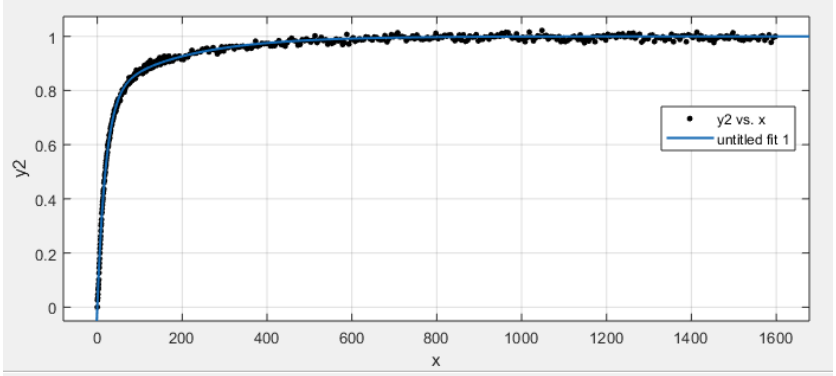

20 % PEG, 225 mM NaCl

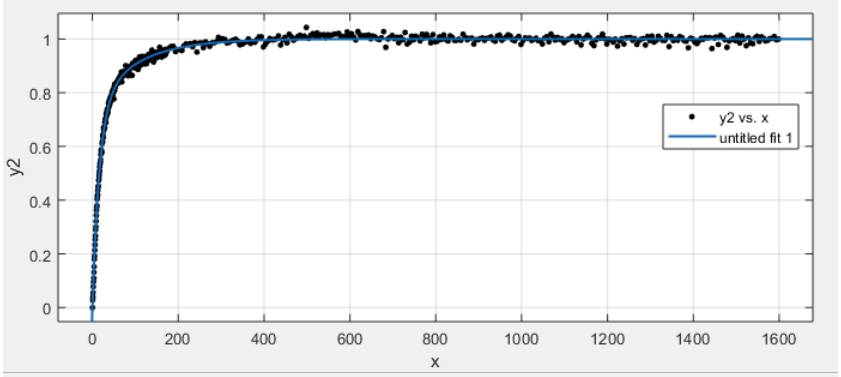

20 % PEG, 300 mM NaCl

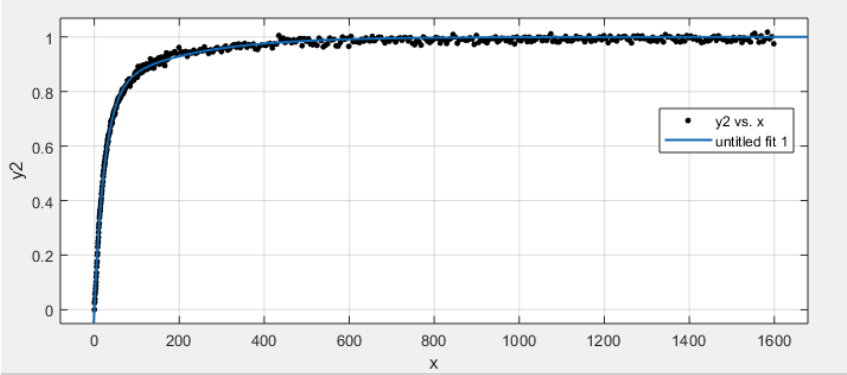

30 % PEG, 75 mM NaCl

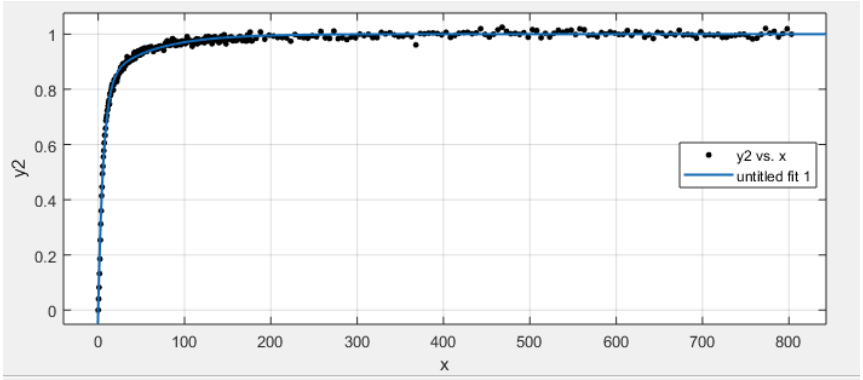

30 % PEG, 150 mM NaCl

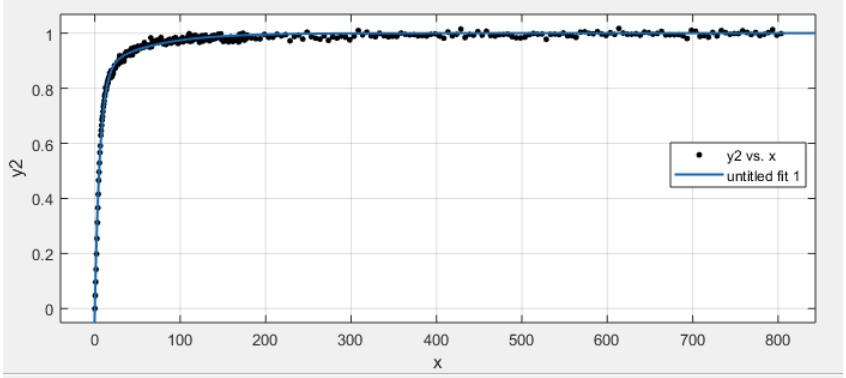

30 % PEG, 225 mM NaCl

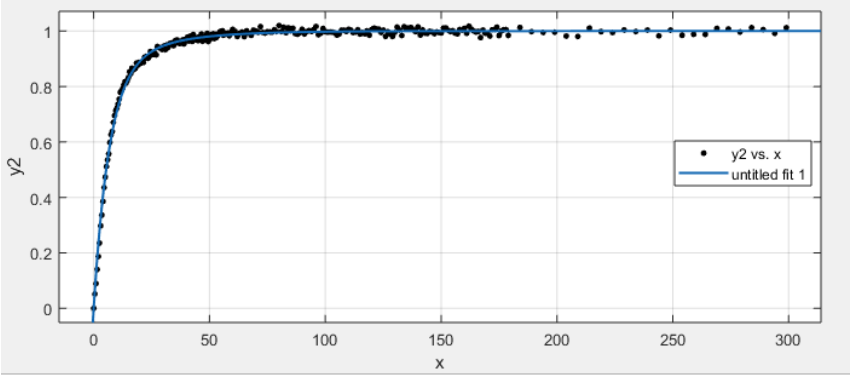

30 % PEG, 300 mM NaCl

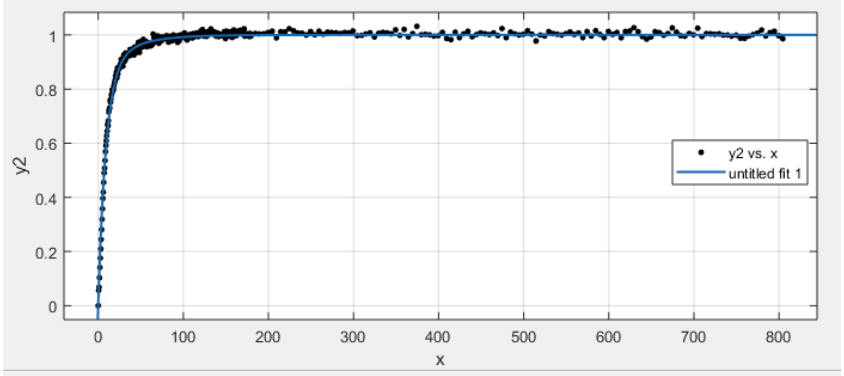

40 % PEG, 75 mM NaCl

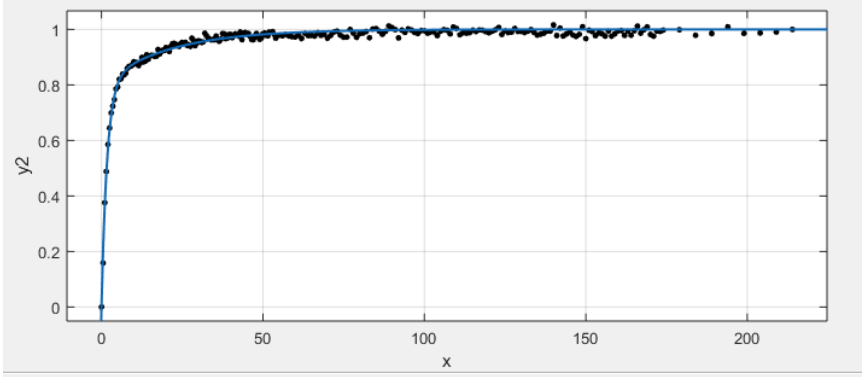

40 % PEG, 150 mM NaCl

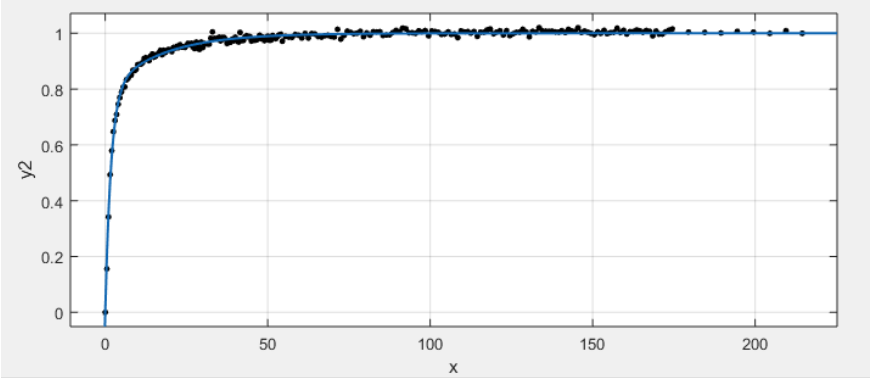

40 % PEG, 225 mM NaCl

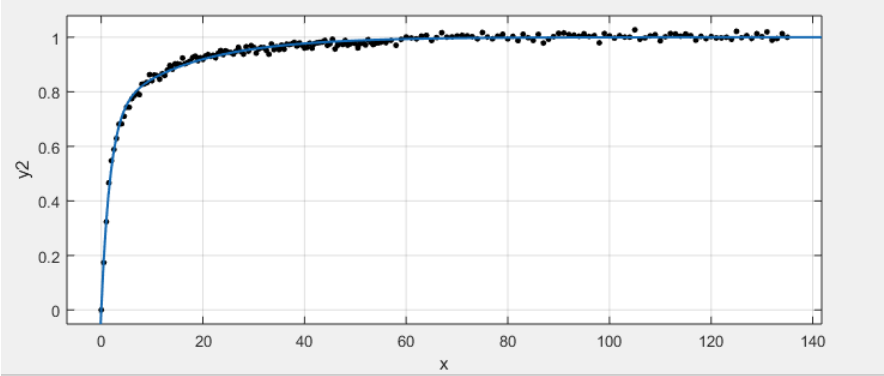

5. Thread-intercalation in dioxane, diglyme, glycerol, PVA, and dextran

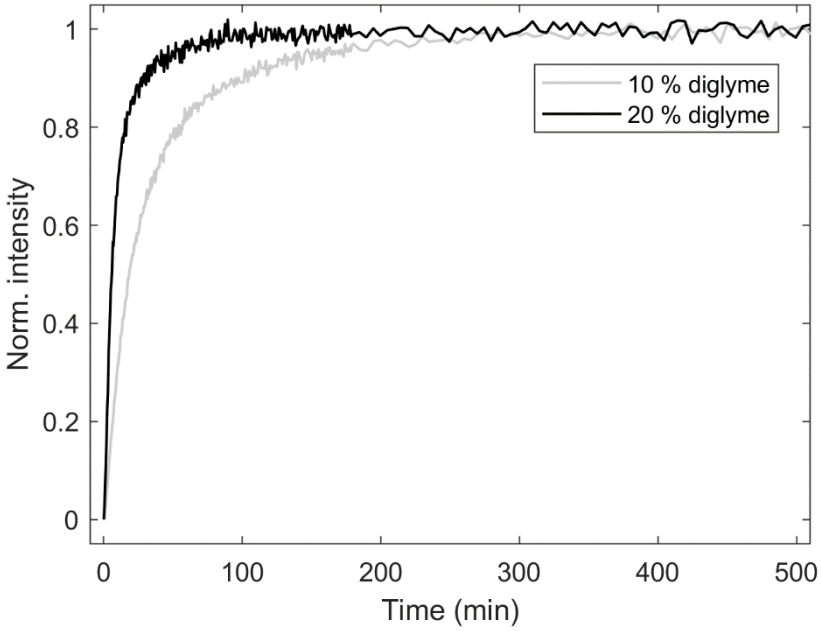

Fig. S6. Thread-intercalation kinetics in diglyme. Fitting the same model as used for PEG, we obtain for 10 % diglyme [A = 0.7052, k = 0.05427, m = 0.01134] and for 20 % diglyme [A = 0.8403, k = 0.1438, m = 0.0227]. TE buffer, 75 mM NaCl, 50 °C.

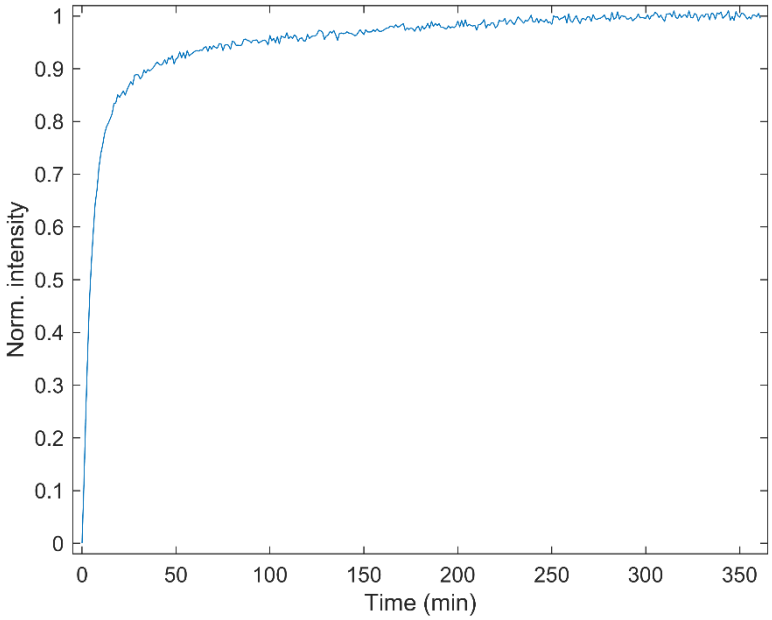

Fig. S7. Thread-intercalation kinetics in 20 % dioxane (1,4-dioxane, pro analysi, Merck). Fitting the same model as used for PEG, we obtain A = 0.8462, k = 0.1848, m = 0.01205. TE buffer, 75 mM NaCl, 50 °C.

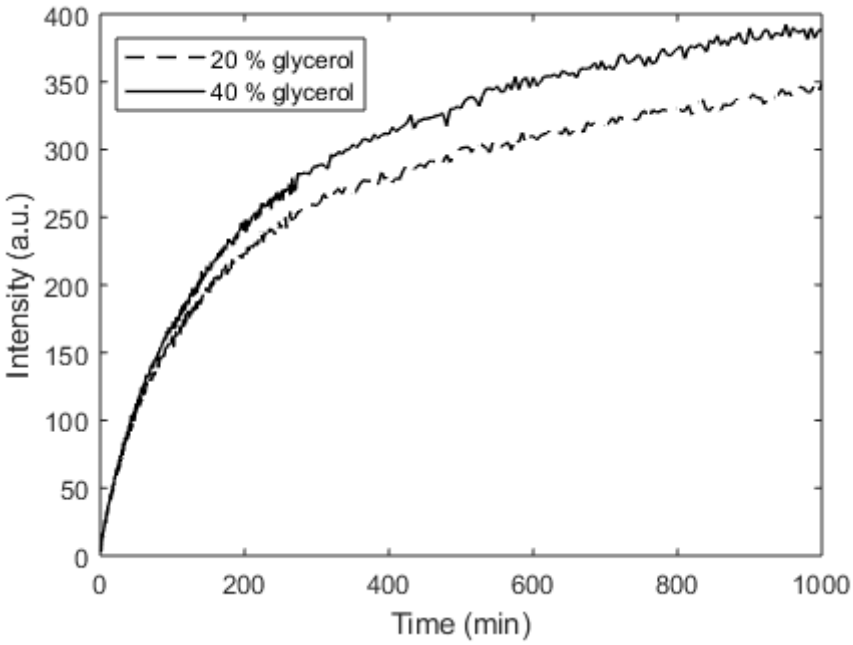

Fig. S8. Thread-intercalation kinetics in glycerol. The data is not normalized because the reaction did not complete within reasonable time. TE buffer, 75 mM NaCl, 50 °C.

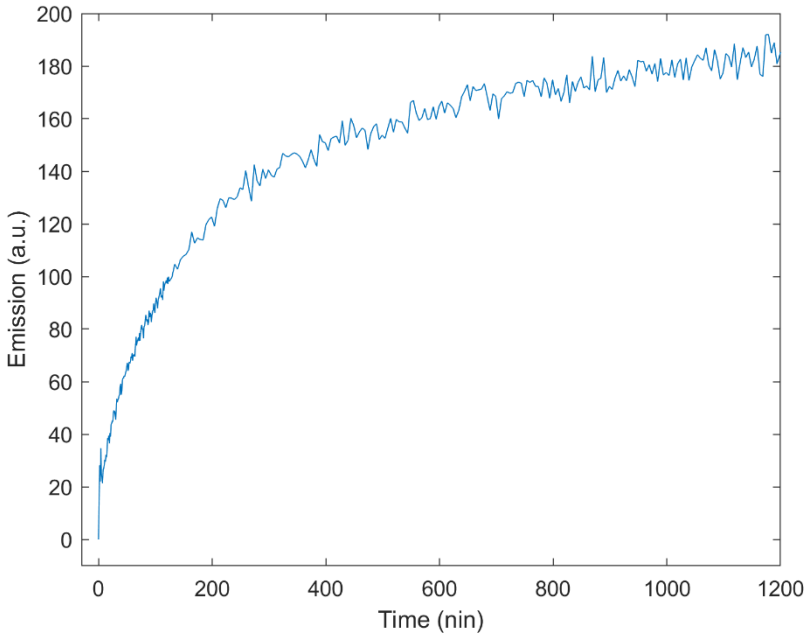

Fig. S9. Thread-intercalation kinetics in 10 % (w/w) poly(vinyl alcohol), average MW = 80 000, purchased from Du Pont (Sweden) under the commercial name Elvanol. The data is not normalized because the reaction did not complete within reasonable time. TE buffer, 75 mM NaCl, 50 °C.

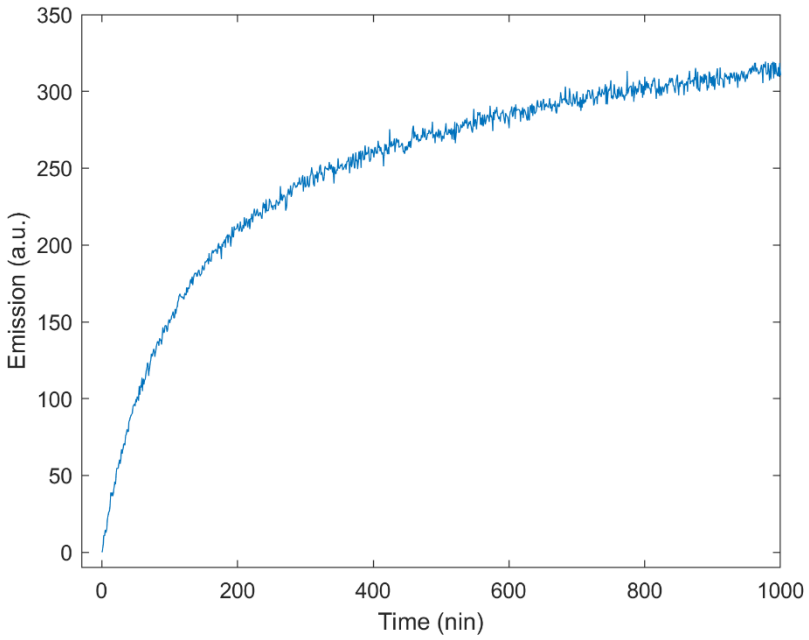

Fig. S10. Thread-intercalation kinetics in 20 % (w/w) dextran from Leuconostoc spp. (average MW 6 000, Sigma). The data is not normalized because the reaction did not complete within reasonable time. TE buffer, 75 mM NaCl, 50 °C.

6. Glyoxal reactions

Glyoxal reacts specifically with single strands. Hyperchromicity at 260 nm shows denaturation; increased absorbance above 300 nm (outside DNA peak) indicates formation of guanine-glyoxal adduct. 60 mM glyoxal, 50 mM NaCl in water, 50 °C.

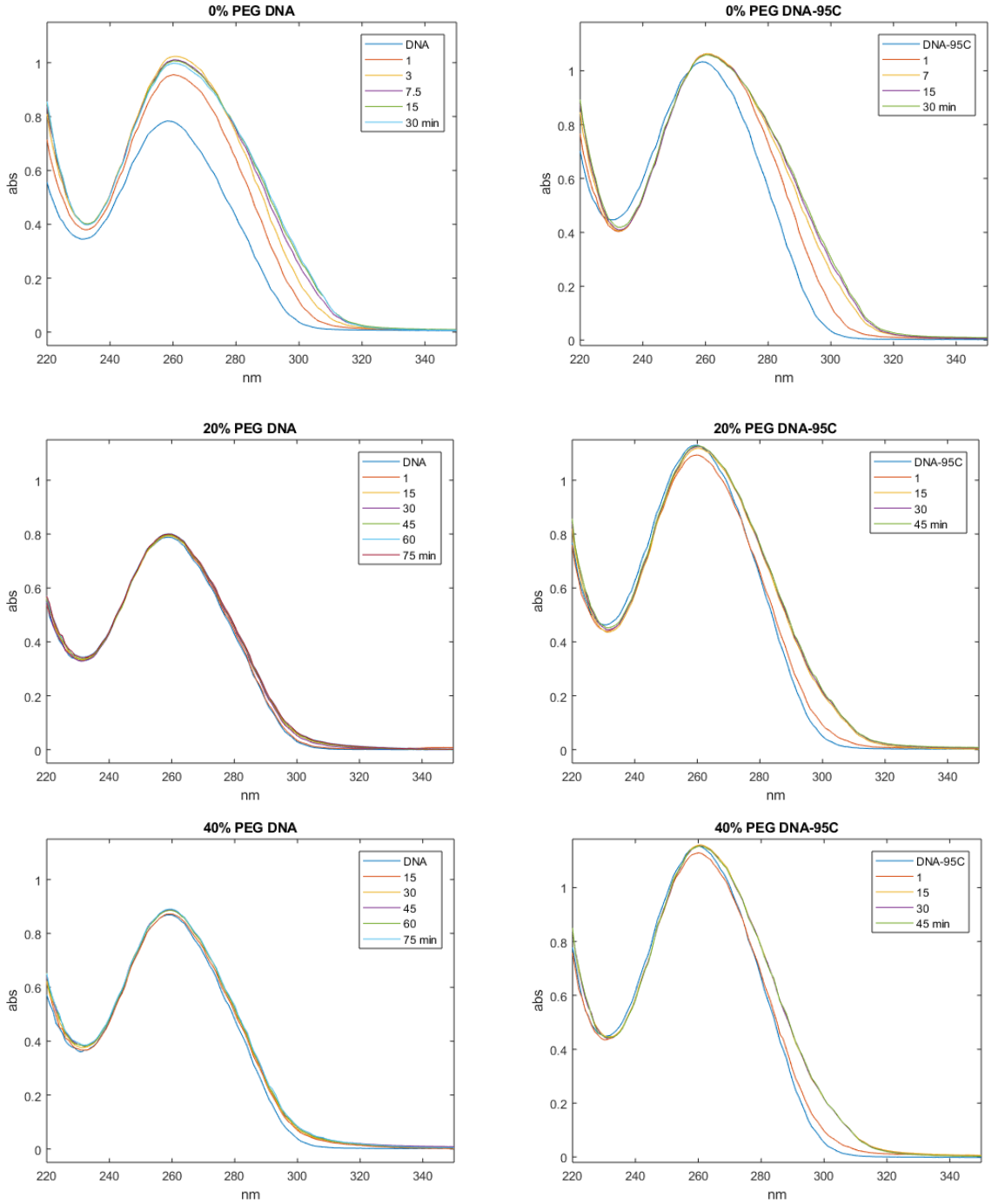

Fig. S11. Left column: Glyoxal immediately reacts with ctDNA due to transient unpaired bases (breathing). Only trace amounts of adduct appears in 20 and 40 % PEG-400. **Right column:** DNA pre-heated to 95 °C and ice quenched to generate single strands; PEG does not inhibit glyoxal reactivity. Concentrations differ between samples due to evaporation.

10 % diglyme, 20 mM glyoxal

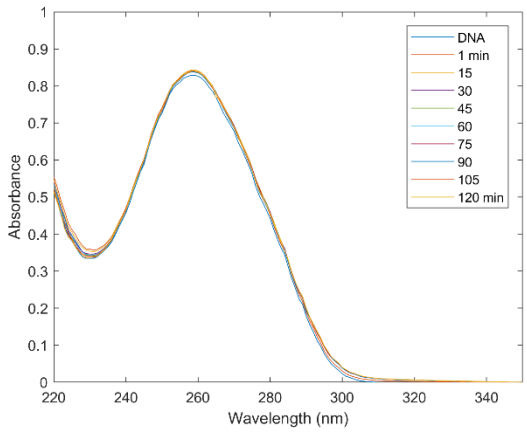

10 % diglyme, 40 mM glyoxal

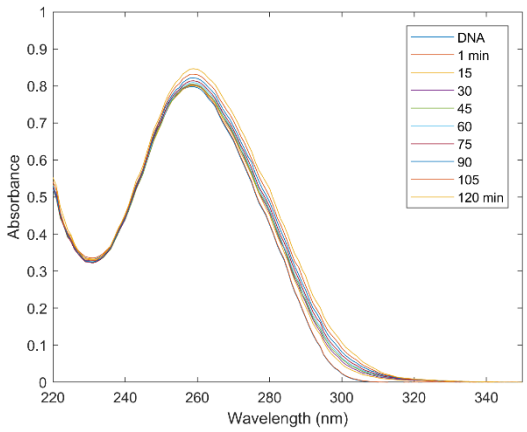

20 % diglyme, 20 mM glyoxal

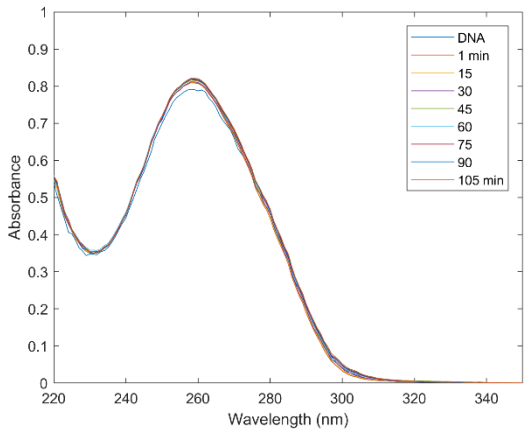

20 % diglyme, 40 mM glyoxal

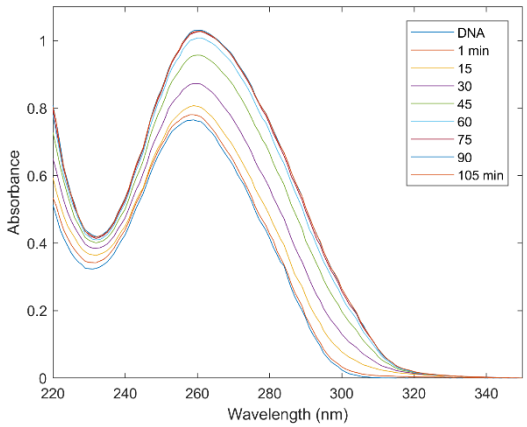

Fig. S12. Diglyme does not protect DNA from glyoxal as well as PEG, but no significant reaction observed for 20 mM glyoxal in 10 and 20 % diglyme. 40 mM glyoxal shows very slow unfinished reaction in 10 % diglyme, and slow reaction in 20 % diglyme. 75 mM NaCl in water, 50 °C.

7. Linear dichroism of DNA in diglyme, glycerol, PEG and TE buffer

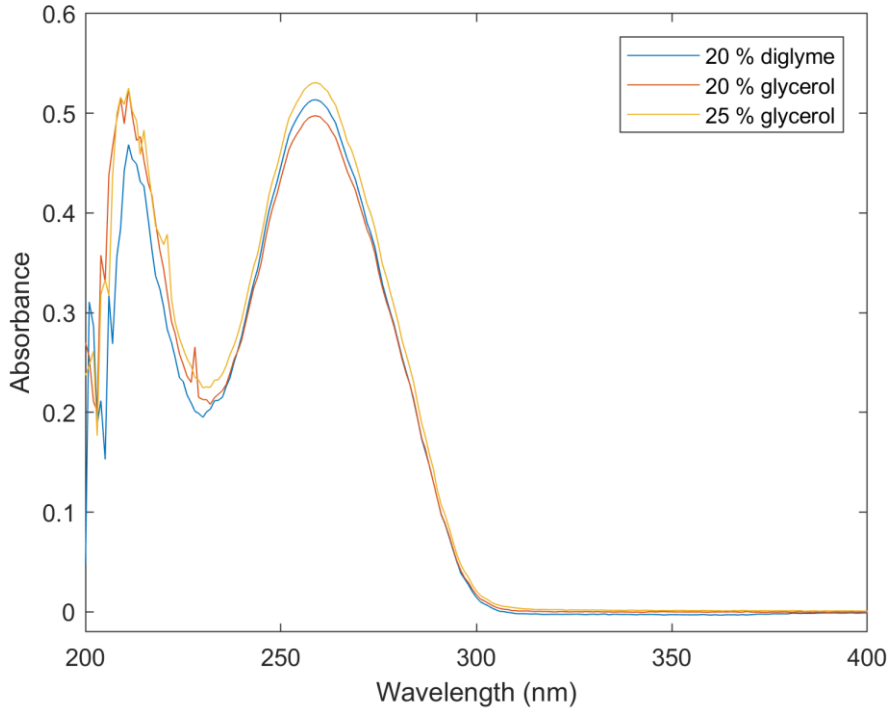

Fig. S13. Ordinary (isotropic) 1 cm absorbance of DNA in diglyme and glycerol using unpolarized light (A_{iso}). Note that the path length in LD measurements is 1 mm. Samples were prepared separately with slightly different concentrations; spectra do not reflect any DNA hyperchromicity.

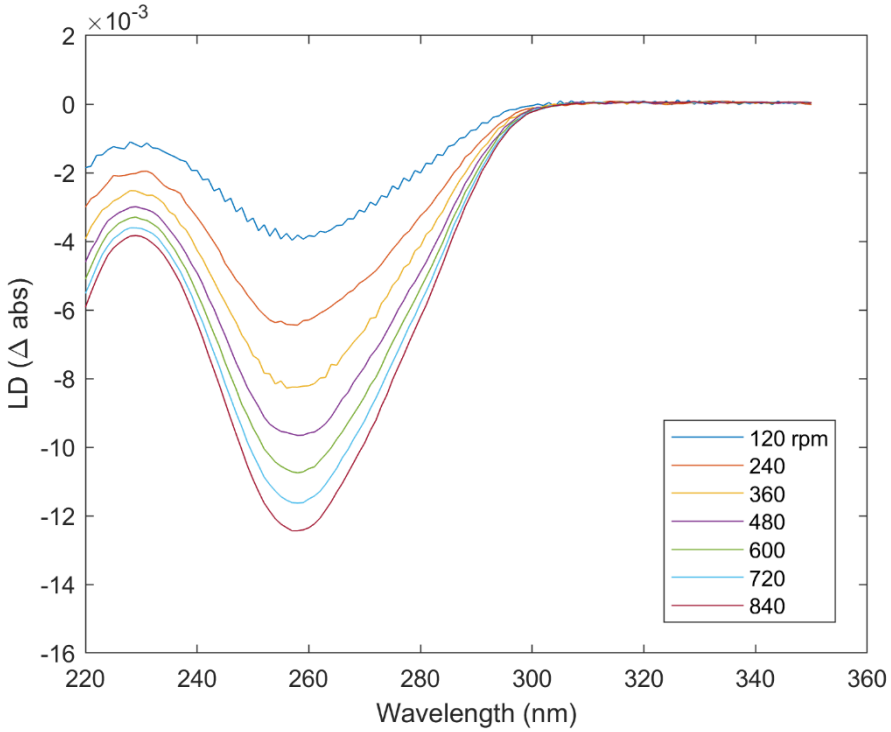

Fig. S14. Linear dichroism of DNA in 20 % diglyme at various couette cell rotation speeds.

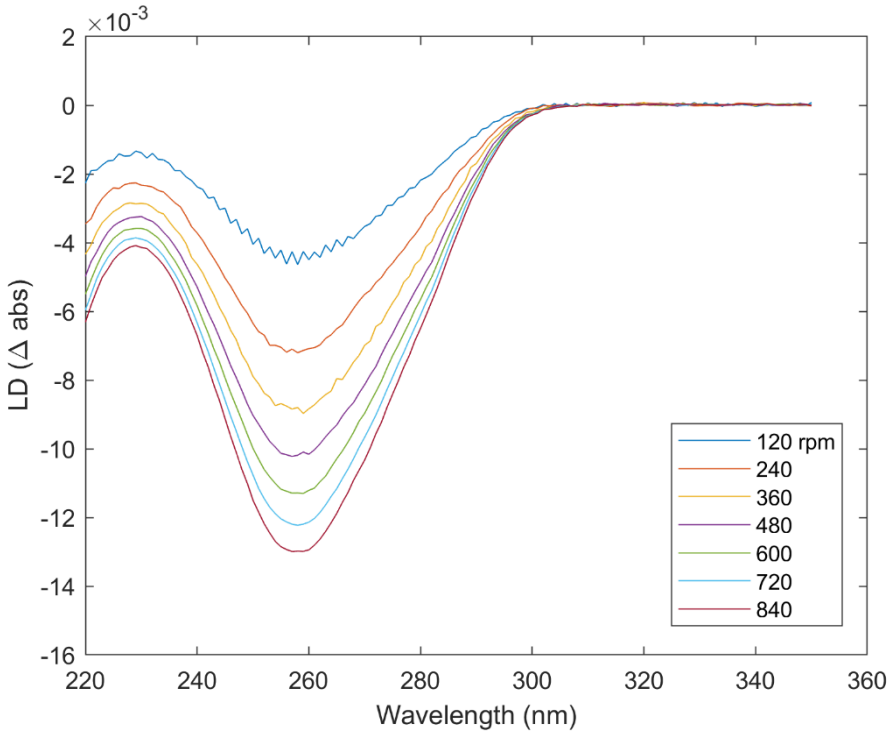

Fig. S15. Linear dichroism of DNA in 20 % glycerol at various couette cell rotation speeds.

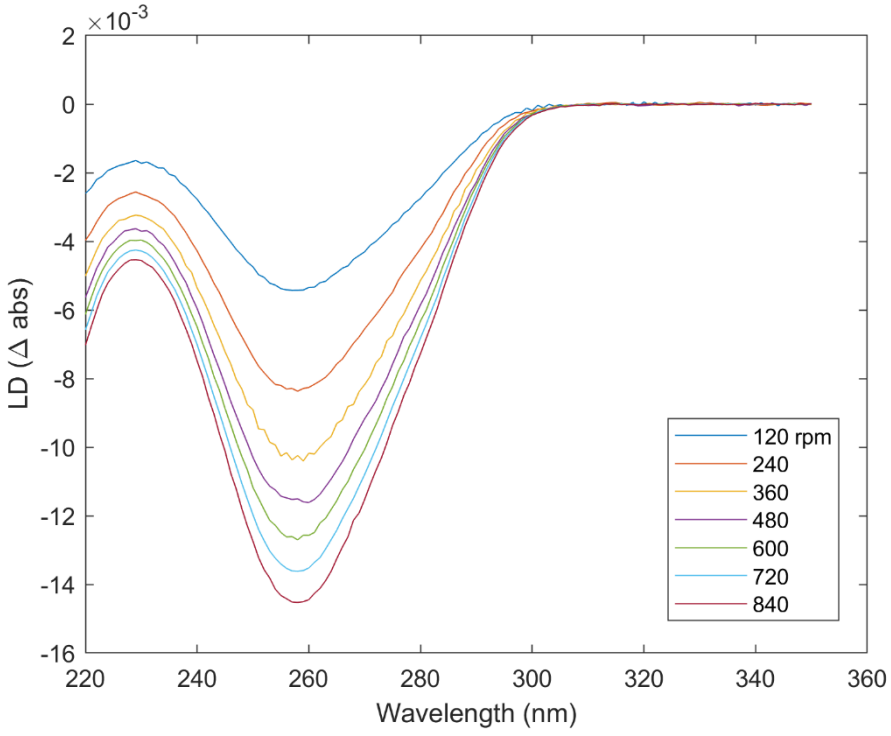

Fig. S16. Linear dichroism of DNA in 25 % glycerol at various couette cell rotation speeds.

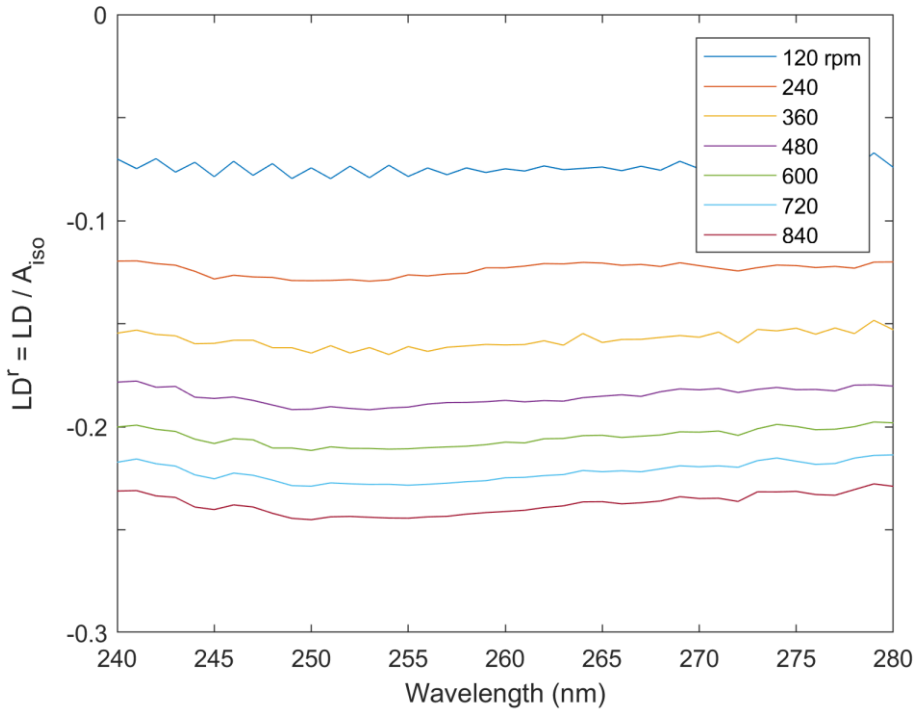

Fig. S17. Reduced linear dichroism ($LD^r = LD / A_{iso}$) of DNA in 20 % diglyme.

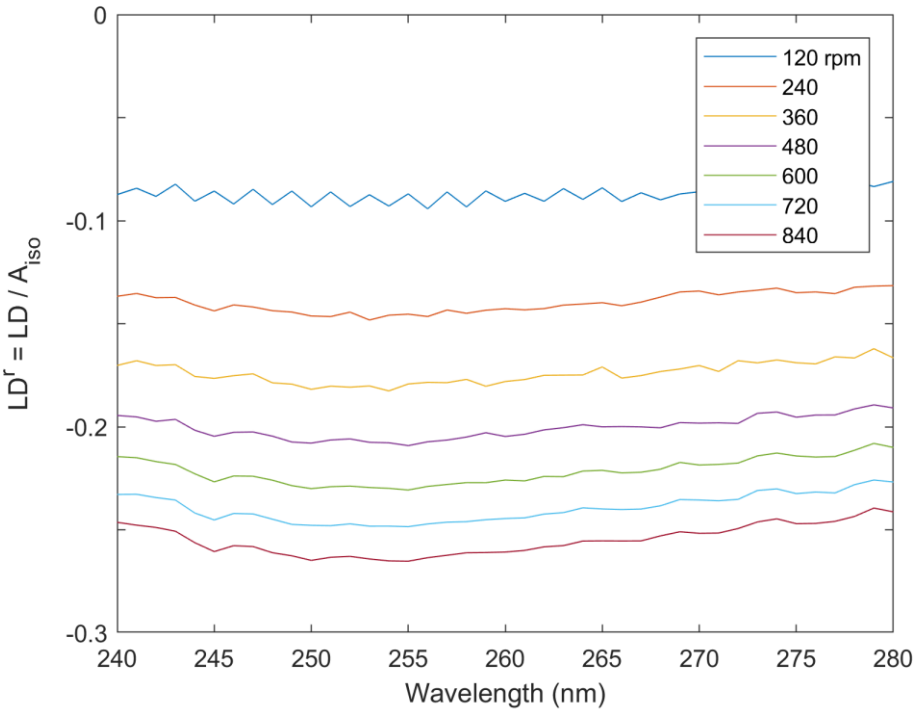

Fig. S18. Reduced linear dichroism ($LD^r = LD / A_{iso}$) of DNA in 20 % glycerol.

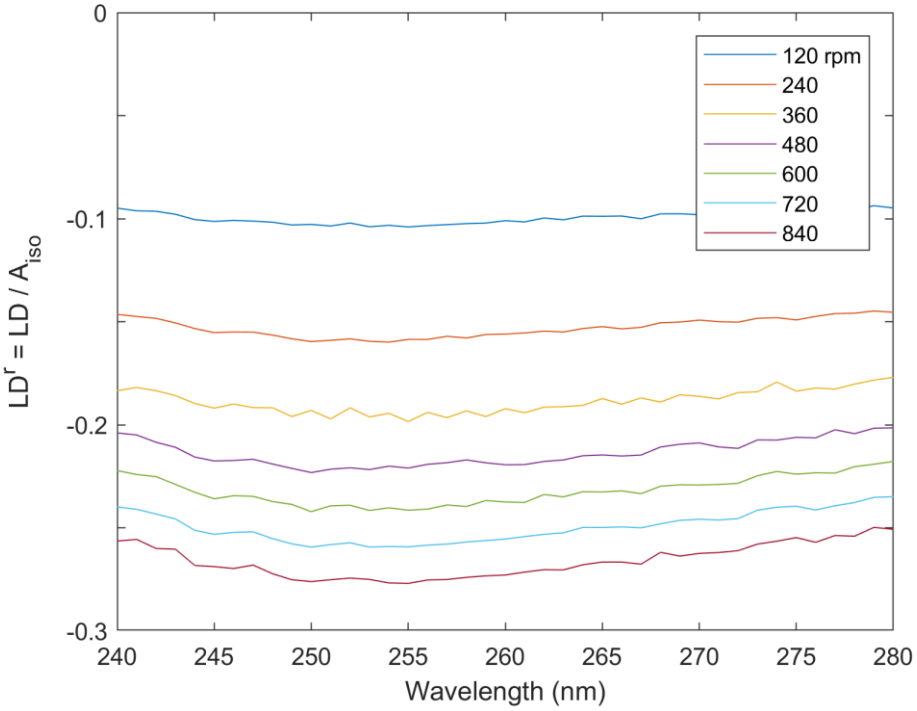

Fig. S19. Reduced linear dichroism ($LD^r = LD / A_{iso}$) of DNA in 25 % glycerol.

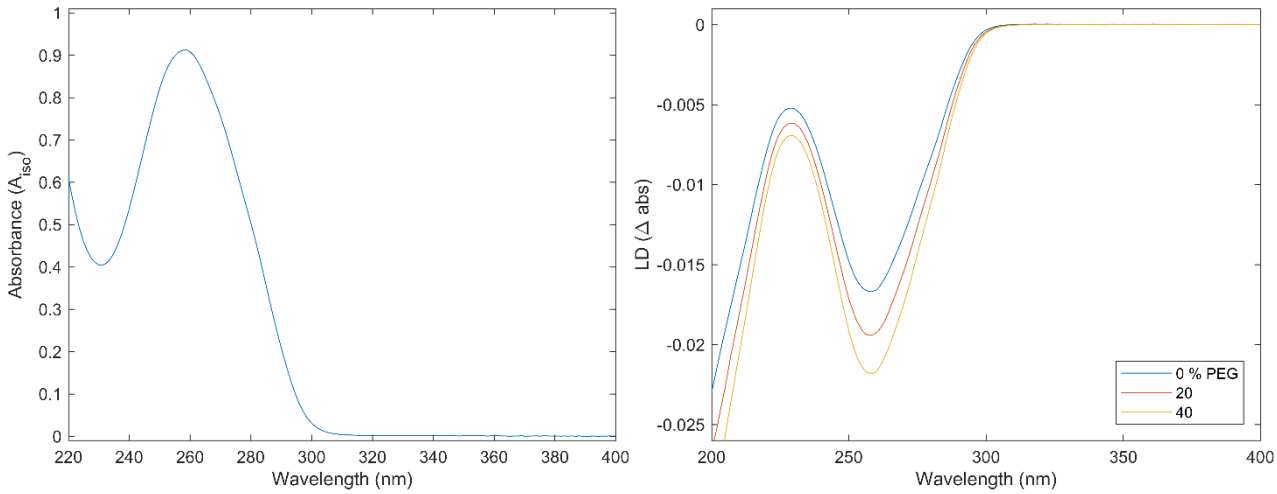

Fig. S20. Absorbance (1 cm in TE buffer) and LD of ctDNA in 0-40 % PEG-400.

8. Hyperchromicity - theory

The hyperchromicity, i.e. increase of absorptivity because of unstacking of nucleobases, is removal of hypochromicity. The hypochromicity H is a lowered-absorptivity effect due to non-degenerate exciton interactions between the transition moment responsible for the observed absorption and involves all transitions of surrounding bases

$$H(\theta, \varphi, \alpha, R_{AB}) = K\,\Sigma[\alpha_A \cos^2(\theta+\varphi) + \alpha_B \sin^2(\theta+\varphi)]\frac{2}{R_{AB}^3} \qquad (1)$$

where K is a constant and θ is the angle between the light-absorbing transition moment in base A and a transition moment in an adjacent stacked base B, α_A and α_B are the polarizabilities at the frequency considered along the two principal axes e_A and e_B in the plane of base A and B, respectively. The angle ϕ is between the transition moment of base B and e_A. The summation is over all base combinations A, B and all transition moments.

If the inter-base distance R_{AB} can be assumed the same for all bases, we have for the difference in oscillator strength between monomer and dimer:

$$f_M - f_D = K\langle[\alpha_A \cos^2(\theta+\varphi) + \alpha_B \sin^2(\theta+\varphi)]\rangle\frac{2}{R_{AB}^3} = \frac{K'}{R_{AB}^3} \qquad (2)$$

where the new constant K' includes some average polarizability α and f_D and f_M being the oscillator strengths of stacked dimer and monomer base, respectively, K' is approximately unity. K' may be calibrated to provide:

$$\text{hyperchromicity } \% = K'\left(1 - \frac{f_D}{f_M}\right) \times 100\ \% \qquad (3)$$

Unstacking generally involves unwinding and thus change of distribution of θ and ϕ values. However, this effect is generally negligible compared to the R_{AB} change due to the inverse cube power dependence in Eq (2).

It is possible to very roughly estimate the ratio of unstacked holes to bases by observing the hyperchromicity of DNA. A hyperchromicity of 3.5 % is 0.0875 of the maximum possible amount of 40 % upon complete denaturation, which we assume is entirely due to base unstacking and losing the coupling between transition moments. We also assume that a base bordering a hole has the same absorption coefficient as a single nucleobase, using the observation that a dinucleotide exhibit almost no hyperchromicity upon heat denaturation (14). Since every hole transforms two stacked nucleobases into bases bordering a hole (as long as the total number of holes is small), the above mentioned 0.0875 is halved into 0.0437 holes per base. In other words, in 20 % PEG, where 3.5 % hyperchromicity is observed, there are about 4 holes in every DNA sequence 100 bases long at any instant. This estimate is probably higher than the real value, ignoring other causes of hyperchromicity such as partial unstacking.

9. Tables

Table S1. Melting temperatures of ctDNA (T_m °C) for various PEG and salt concentrations in Fig 2b. Additional salt compensates for a decreased melting temperature in the presence of PEG but does not inhibit threading intercalation.

	[NaCl]			
PEG %	**75 mM**	**150 mM**	**225 mM**	**300 mM**
0	81.5	86.5	87.5	n.d.
10	79.5	84.5	86.5	87.5
20	78.5	82.5	84.5	85.5
30	77.5	81.0	83.0	83.5
40	75.5	77.5	78.5	n.d.

n.d. = not determinable due to too high temperature or to precipitation in PEG

Table S2: Mechanical properties of DNA in the absence or in the presence of diglyme.

	$\boldsymbol{F}$ (pN)$^{+}$	$\boldsymbol{\sigma_F}$ (pN)	$\boldsymbol{P}$ (nm)*	$\boldsymbol{\sigma_P}$ (nm)	$\boldsymbol{S}$ (pN)*	$\boldsymbol{\sigma_S}$ (pN)	$\boldsymbol{L_c}$ (nm)*	$\boldsymbol{\sigma_{L_c}}$ (nm)	$\boldsymbol{r}$ (Å)$^{++}$	N**
Buffer	59.7 ±0.3	1.1	44.7 ±0.7	5.0	366.0 ±4.0	27.4	2.05 ±0.01	0.1	14.2 ±0.1	48
+ 10% diglyme	50.3 ±0.4	1.3	40.9 ±0.8	5.2	464.5 ±5.5	36.2	2.06 ±0.01	0.1	12.0 ±0.1	44
+ 20% diglyme	40.4 ±0.3	1.3	46.6 ±1.1	7.1	663.5 ±18.1	119.0	2.02 ±0.01	0.1	10.7 ±0.2	43
Buffer ***	59.8 ±0.3	1.2	42.7 ±0.8	5.4	333.5 ±2.2	14.5	2.06 ±0.01	0.1	14.4 ±0.1	42

$^{+}$ Overstretching force. The value refers to first rupture of overstretching transition.

$^{++}$ The hydrodynamic B-DNA radius r (Å) was calculated as $r = \sqrt{4Pk_BT/S}$.

* P is persistent length, S is stretch modulus and L_c is contour length. P, S and L_c are obtained from the fitting of eWLC model to DNA pulling curves below 25-35pN.Values are: mean ± SEM (standard error of the mean), being $SEM = \sigma_x/\sqrt{N}$.

** Number of DNA molecules.

*** DNA preincubated in 20 % diglyme + 20 mM glyoxal and 50mM NaCl at room temperature for 1 h.

9. References

1. Andersson J., Li M., & Lincoln P. (2010) AT-specific DNA binding of binuclear ruthenium complexes at the border of threading intercalation. *Chemistry - A European Journal* 16(36):11037-11046.

2. Berman H. M. & Schneider, B. (1999) Nucleic acid hydration. In Neidle, S. (ed.), *Oxford Handbook of Nucleic Acid Structure*, (Oxford University Press, New York), pp 295–312.

3. Friedman A. E., Chambron J. C., Sauvage J. P., Turro N. J., & Barton J. K. (1990) A molecular light switch for DNA: Ru(bpy)2(dppz)2+. *Journal of the American Chemical Society* 112(12):4960-4962.

4. Nordén B. & Seth S. (1979) Structure of strand-separted DNA in different environments studied by linear dichroism. *Biopolymers* 18(9):2323-2339.

5. Schellman J. A. (1974) Flexibility of DNA. *Biopolymers* 13(1):217-226.

6. Wilson R. W. & Schellman J. A. (1978) The flow linear dichroism of DNA: Comparison with the bead-spring theory. *Biopolymers* 17(5):1235-1248.

7. Nordell P., *et al.* (2008) DNA polymorphism as an origin of adenine-thymine tract length-dependent threading intercalation rate. *Journal of the American Chemical Society* 130(44):14651-14658.

8. Moffitt J. R., Chemla Y. R., Izhaky D., & Bustamante C. (2006) Differential detection of dual traps improves the spatial resolution of optical tweezers. *Proceedings of the National Academy of Sciences of the United States of America* 103(24):9006-9011.

9. Bustamante C., Chemla Y. R., & Moffitt J. R. (2009) High-resolution dual-trap optical tweezers with differential detection: Data collection and instrument calibration. *Cold Spring Harbor Protocols* 4(10).

10. Landry M. P., McCall P. M., Qi Z., & Chemla Y. R. (2009) Characterization of photoactivated singlet oxygen damage in single-molecule optical trap experiments. *Biophysical Journal* 97(8):2128-2136.

11. Petrosyan R. (2017) Improved approximations for some polymer extension models. *Rheologica Acta* 56(1):21-26.

12. Nyberg L., Persson F., Åkerman B., & Westerlund F. (2013) Heterogeneous staining: A tool for studies of how fluorescent dyes affect the physical properties of DNA. *Nucleic Acids Research* 41(19).

13. Persson F. & Tegenfeldt J. O. (2010) DNA in nanochannels - Directly visualizing genomic information. *Chemical Society Reviews* 39(3):985-999.

14. Fornasiero D. (1981) Studies of vibronic exciton interactions between pairs of chromophores. PhD thesis, University of Adelaide, Adelaide, Australia.